

We are IntechOpen, the world's leading publisher of Open Access books Built by scientists, for scientists

6,900

Open access books available

186,000

International authors and editors

200M

Downloads

Our authors are among the

154

Countries delivered to

TOP 1%

most cited scientists

12.2%

Contributors from top 500 universities



WEB OF SCIENCE™

Selection of our books indexed in the Book Citation Index
in Web of Science™ Core Collection (BKCI)

Interested in publishing with us?
Contact book.department@intechopen.com

Numbers displayed above are based on latest data collected.
For more information visit www.intechopen.com



The Use of Industrial Waste for the Bioremediation of Water Used in Industrial Processes

*Rosa Hernández-Soto, José A. Hernández,
Alba N. Ardila-Arias, Mercedes Salazar-Hernández
and María del Carmen Salazar-Hernandez*

Abstract

Recently the interest in the remediation of liquid effluents from industries such as paint manufacturing, leather tanning, etc. has increased, because the quality of the water used in these processes is highly compromised and is generally discarded without any process of purification, causing an inadequate use of water and contributing to the hydric stress of the planet. Therefore, it is necessary to find alternatives for the remediation of water used in industrial processes; one of the methods that has been widely accepted given its high efficiency, low cost, and versatility compared to others is the bioadsorption using materials derived from various processes used for the elimination of metals such as Cr, Co, Cu, Ni, etc. from liquid effluents. Among the materials used for this purpose are rice husk, orange, and wheat as well as apatite (hydroxyapatite and brushite), derived from animal bones, which have shown good capacity (>90%) to adsorb metals from aqueous solutions. Through the characterization by DRX, FTIR, and SEM, of the brushite and studies in equilibrium and kinetics of adsorption, it has been demonstrated that this material has a good capacity to remove metals present in water.

Keywords: brushite, removal, isotherm, kinetics, metals

1. Introduction

The contamination of water bodies due to the presence of heavy metals is a serious problem, because every day this vital resource is scarce and because of the high toxicity of these compounds for the health of living beings. The metals present in water are a risk factor for the development of diseases such as cancer and dermatitis; in addition, they may be accumulated in the human body because they cannot be metabolized [1–7]. Solid-liquid removal processes such as chemical precipitation, filtration, and adsorption, among others, have been widely used for the removal of metals such as nickel (Ni), iron (Fe), copper (Cu), zinc (Zn), cobalt (Co), and chromium (Cr) of liquid effluents [8–11]; however, some of these methods have disadvantages such as high operating cost and low efficiency; however, methods such as coagulation and precipitation are already used in various industrial processes for the removal of metals from industrial effluents [12]. In recent years, adsorption has

been one of the most used metal ion removal techniques, since it is a simple, effective, and inexpensive process compared to other methods [13–17]. Adsorption processes have been experimented with an extensive amount of materials such as adsorbents, among which activated carbon stands out due to its high capacity for capturing metal ions; however, this material has the disadvantage of generating large quantities of sludge, since the removal of metals trapped in activated carbon can only be done with processes that are often expensive such as leaching [5, 9, 18, 19]. For this reason, the use of different materials that are economical, are easy to obtain, and have high efficiency in the removal of metal ions has been investigated. In recent decades, these studies have focused on the waste derived from the agricultural industry that produces large amounts of waste such as biomass, wheat husks, rice, orange, etc. [2, 4, 8, 9, 16, 18–30]; the use of residues from other industries has also been investigated, such as the case of apatites derived from the bone tissue of animals, which have been used for removal of dyes and metal ions obtaining promising results. The use of apatites in particular hydroxyapatite and brushite for the adsorption of heavy metals such as Cd, Cu, Ni, Pb, Co, Mn, and Fe, to name a few, has already been reported [31–35]; however, in most of the studies carried out, only the process of adsorption of metallic solutions of a single component has been analyzed, so the objective of the present work is to evaluate the capacity of brushite (nDCPD), obtained from bovine bone to remove Ni (II), Co (II), and Cu (II) of aqueous solutions, analyzing the selectivity of removal of metal ions in aqueous solutions with two or three different metals, determining the kinetic models and in equilibrium in which the removal of metals takes place and the structural changes suffered by nDCPD during the development of the different tests.

2. Experimental

2.1 Reagents

All the reagents that were used were of analytical grade. The water used for the preparation of solutions in the experiment was deionized. The solutions to be evaluated were prepared by dissolution of salts of nickel ($\text{Ni}(\text{NO}_3)_2 \cdot 6\text{H}_2\text{O}$), cobalt ($\text{Co}(\text{NO}_3)_2 \cdot 6\text{H}_2\text{O}$), and copper ($\text{Cu}(\text{NO}_3)_2$) in concentrations from 0 to 1,000 ppm.

2.2 Preparation of the adsorbent

Brushite natural (nDCPD) was obtained from bovine bone, which was washed with hot water several times to remove tissue debris, and then it was dried at 353 K for 24 h. Next, the bones were crushed and sieved to obtain a particle size of 150 mesh (104 μm). Then, the powder obtained was treated with HCl and NaOH solution, 10^{-2} M, respectively, using a ratio of 30% w/v. Finally nDCPD was stored until its use [1].

2.3 Characterization of natural brushite

The X-ray diffraction patterns (XRD) were obtained in a Rigaku diffractometer (Ultima IV). The Fourier transform infrared studies of the samples were performed in an IR 100 Analyzer spectrophotometer (PerkinElmer), in a range of 400–4000 cm^{-1} . The scanning electron microscopy (SEM) images were obtained in a JOEL equipment (6510-Plus).

2.4 Co, Cu, and Ni adsorption isotherm

The different isotherm models used to describe the adsorption of Ni, Co, and Cu are concentrated in **Table 1**, for each one of the regression coefficients was

calculated to evaluate the adjustment of each nonlinear model and the separation factor, R_L , which allows to predict the affinity between the adsorbent and adsorbate, using Eq. 1 [5]:

$$R_L = \frac{1}{1 + K_L C_0} \quad (1)$$

where K_L is the constant of the Langmuir model and C_0 is the initial concentration of Ni, Co, and Cu ions. To know the thermodynamics of the adsorption process, the free-energy parameters of apparent Gibbs were determined. ΔG (kJ/mol), ΔH (kJ/mol), and ΔS (kJ/mol K), which are directly related to changes in temperature, and help to understand the mechanism of adsorption of metal ions, by using Eqs. 2, 3, and 4 [27, 36]:

$$\Delta G = -RT \ln(k) \quad (2)$$

$$k = 55.5 K_L \quad (3)$$

$$\ln(k) = -\frac{\Delta H}{RT} + \frac{\Delta S}{R} \quad (4)$$

where K_L is the constant of the Langmuir model (L/mol), R is the constant of the ideal gases, and T is the absolute temperature (K). The values of ΔH and ΔS can be determined with the slope and ordered to the origin of the graph $\ln k$ as a function of $1/T$.

For the study of the adsorption isotherms of the different metals in nDCPD, 1 g of sorbent was put in contact with 50 ml of the aqueous solution of the metal ions Co, Cu, and Ni, varying the concentration between 0 and 1000 ppm in a shaker (ZHWHY-200D) with an agitation of 200 rpm at 25, 35, and 45°C for 24 h of contact time.

2.5 Batch removal kinetics

The experiments to establish the kinetics of metal ion removal in nDCPD and to know the evolution of the adsorption of Ni, Co, and Cu ions in the biomaterial were carried out in batches. They were carried out varying the concentration of nDCPD (C_{ads}), from 0 to 40 g/L, during 24 h at a speed of 200 rpm and at 25, 35, and 45°C. At specific times aliquots of aqueous solution were taken to separate the adsorbent material and the liquid supernatant by centrifugation at 10,000 rpm. The supernatant was analyzed with the help of a spectrophotometer (JENWAY 6705) to know the concentration of the different ions present in the solution. The amount of ions removed (q_e) by nDCPD was obtained by applying Eq. 5 [4]:

$$q_e = \frac{V(C_0 - C)}{m} \quad (5)$$

where C_0 and C represent the initial concentration and the concentration at time t or in equilibrium (mg/L), V is the volume of solution (L), and m is the mass of nDCPD (g).

The percentage of removal (%R) was calculated as Eq. 6 [5]:

$$\%R = \frac{(C_0 - C_e)}{C_0} \times 100 \quad (6)$$

Model	Equation
SIPS	$q_e = \frac{q_m (K_S C_e)^{n_S}}{1 + (K_S C_e)^{n_S}}$
Redlich-Peterson (R-P)	$q_e = \frac{K_R C_e}{1 + a_R C_e^\beta}$
Langmuir	$q_e = \frac{q_m K_L C_e}{1 + K_L C_e}$
Temkin	$q_e = A + B \ln(C_e)$
Freundlich	$q_e = K_F C_e^{1/n}$

SIPS: K_S (L/mg), q_m (mg/g), n_S (dimensionless); Redlich-Peterson: K_R (L/g), a_R (L/mg) ^{β} , β (dimensionless); Langmuir: K_L (L/mg), q_m (mg/g), R_L (dimensionless); Freundlich: K_F [(mg/g)(L/mg)] ^{$1/n$} , n (dimensionless); Temkin: A (L/mg), B (kJ/mol).

Table 1. Nonlinear adsorption isotherm models [40, 41].

3. Results and discussion

3.1 Adsorption isotherms

Adsorption data obtained at different temperatures help to understand the interaction between nDCPD and Ni, Co, and Cu ions; analyzing the data with different adsorption models, the model with better fit is obtained. In **Table 1**, the most used isotherm models are described according to the literature, and in **Figures 1–3** for Ni, Co, and Cu, respectively, the behavior of the removal of metal ions at different temperatures is shown. The parameters derived from the adjustments together with the coefficient of determination, R^2 , are shown in **Tables 2–4**, for Ni, Co, and Cu, respectively, using the SigmaPlot software (®Version 11) at a temperature of 15, 30, and 45°C. Based on the results obtained, it is observed that the most appropriate models to adjust the adsorption in nDCPD of Ni metal ions, in the three temperatures analyzed (**Figure 1** and **Table 2**), are SIPS, Redlich-Peterson, and Langmuir and Freundlich, suggesting that Ni ions are adsorbed on the surface of nDCPD causing the formation of a monolayer and that the adsorption process is physical. On the other hand, the results obtained in the removal of Co ions (**Figure 2** and **Table 3**), show that the models with the best fit of the data are SIPS, Redlich-Peterson and Langmuir in the three temperatures analyzed, which implies that the cobalt ions are adsorbed on the surface of nDCPD, in a physical process independent of temperature. Finally, in the removal of Cu ions (**Figure 3** and **Table 4**), only an appropriate fit was obtained with the SIPS model, which suggests that the removal of copper ions in equilibrium is carried out by a physisorption process on the surface of the adsorbent. The obtained results also show that the removal of all the ions analyzed using nDCPD is favored given that the R_L values are between 0 and 1, which indicates that the adsorption is favorable; this tendency can be seen independently of the temperature used. The results of metal ion removal obtained in the present study using nDCPD are comparable with those obtained using other agroindustrial residues, since for Ni, removals between 6.88 and 120 mg/g have been obtained, while the value obtained in this work was of 22.48 mg/g. In the case of Co, a removal range of 2.55–45.44 mg/g has been reported, and in our case a value of 41.81 mg/g was obtained, finally, for Cu, removal values have been reported in the range of 0.98–163.01 mg/g, while in the present study a value of 41.88 mg/g of adsorbent was obtained [3–5, 13, 20–23, 26]. On the other hand, when comparing the results obtained with those reported by other authors who also used hydroxyapatites and brushite as adsorbent material, it was observed that the

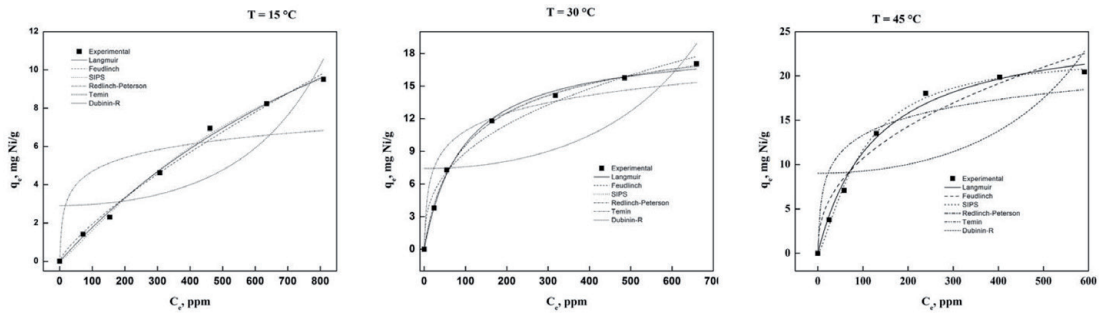


Figure 1. Adjustment of the experimental data of Ni adsorption using the different models of isotherms at different temperatures.

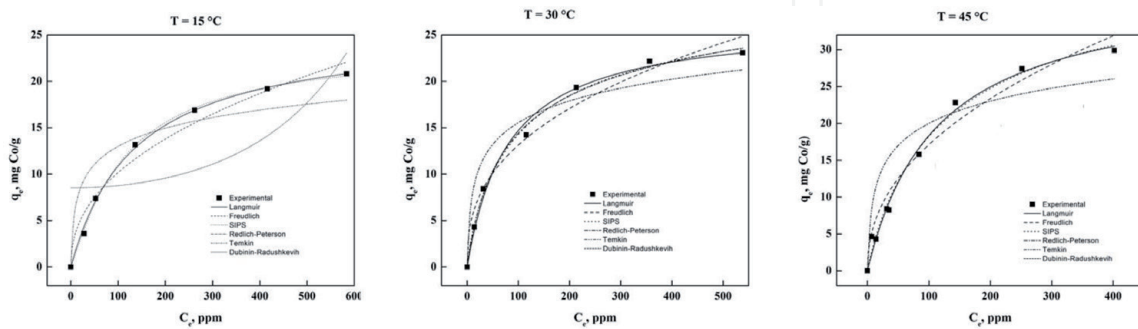


Figure 2. Adjustment of the experimental data of Co adsorption using the different models of isotherms at different temperatures.

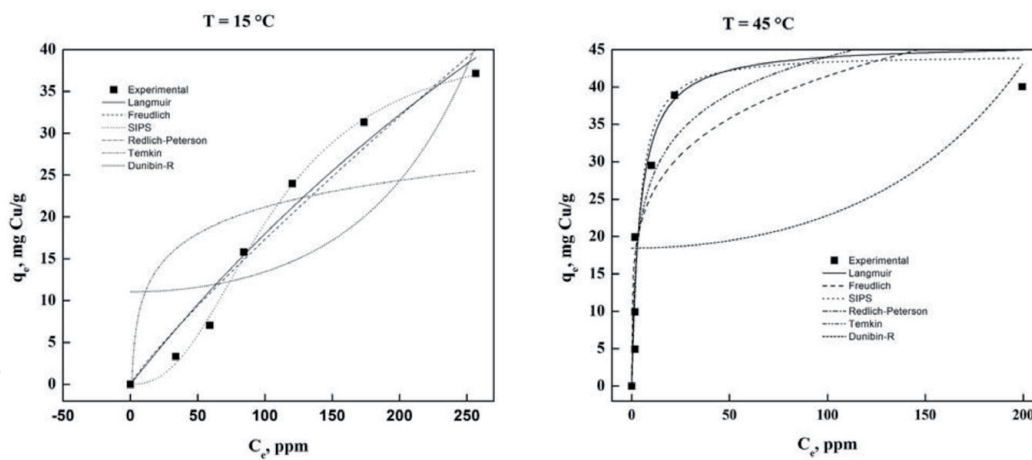


Figure 3. Adjustment of the experimental data of Cu adsorption using the different models of isotherms at different temperatures.

model that was best adjusted was that of Langmuir, with a capacity of Ni adsorption reported between 9.9 and 40.0 mg/g, these data are comparable with those obtained in the present work. In the case of Co, an adsorption with apatites of 8.8–20 mg/g has been reported, a value lower than that obtained with natural nDCPD obtained in the present study, which is 41.8 mg/g. Finally, in the case of Cu ions, a range of adsorption has been documented in this type of materials of 26.6–343.64 mg/g, a value comparable to that obtained in the present work with nDCPD [7, 15, 32–35]. From the results obtained, it can be inferred that brushite is a material with good characteristics for the removal of metals from wastewater; it could also be observed that nDCPD favors the adsorption of Cu over Co and Ni.

Models	Parameters		
	15°C	30°C	45°C
SIPS			
K_S	0.005	0.016	0.0020
q_m	18.2426	20.6152	22.4789
n_S	1.1611	0.8644	1.3671
R^2	0.9969	0.9985	0.9974
Redlich-Peterson			
K_R	0.0191	0.2423	0.2024
a_R	0.007	0.0240	0.0078
β	1.0	0.9046	1.0
R^2	0.9943	0.9990	0.9913
Langmuir			
K_L	0.0007	0.0078	0.0105
q_m	27.7198	18.9551	25.9445
R^2	0.9962	0.9975	0.9913
R_L	0.588–0.935	0.114–0.562	0.087–0.488
Freundlich			
K_F	0.0552	1.6384	1.5515
n	1.2921	2.7263	2.3854
R^2	0.9923	0.9869	0.9980
Temkin			
A	1.873×10^{-8}	2.683×10^{-8}	2.3779×10^{-10}
B	1.0213	2.3617	2.8940
R^2	0.6402	0.9078	0.8337

Table 2.
Equilibrium parameters of adsorption models at different temperatures for Ni ions.

3.2 Effect of temperature on the removal of metal ions

In the literature it has been widely reported that one of the most important variables in the process of solid-liquid removal is temperature, since it directly influences some thermodynamic parameters (Table 5) of great interest in the removal process. The negative values of ΔG indicate that the removal processes of the metal ions of the aqueous solutions are carried out spontaneously; the increase of the value in the negative scale parallel to the increase of the temperature shows the direct dependence with this variable. The positive value of the ΔS indicates that the sites of the solid-liquid interface during the uptake of metal ions increase due to the randomness in the adsorbent [4, 5, 13, 34, 37], while the positive value of ΔH reveals that the process has an endothermic nature, which will influence the increase in ion removal as the temperature increases, which makes the process feasible and spontaneous at temperatures above room temperature [27, 36, 37]. Several reports indicate that the metal adsorption process in brushite is spontaneous; however, some authors indicate that the heat of adsorption in this process is negative, therefore, as the temperature increases, the removal capacity decreases.

Models	Parameters		
	15°C	30°C	45°C
SIPS			
K_S	0.0470	0.0208	0.0117
q_m	23.8607	30.1446	41.8104
n_S	1.1294	0.8178	0.9105
R^2	0.9895	0.9958	0.9895
Redlich-Peterson			
K_R	0.1884	0.4259	0.3462
a_R	0.0073	0.0326	0.0089
β	1.0	0.8886	1.0
R^2	0.9980	0.9953	0.9891
Langmuir			
K_L	0.0073	0.0089	0.0124
q_m	25.6863	26.5263	39.0000
R^2	0.9980	0.9933	0.9891
R_L	0.121–0.578	0.101–0.529	0.075–0.447
Freundlich			
K_F	1.3457	2.2983	2.1685
n	2.2770	2.6411	2.2291
R^2	0.9723	0.9773	0.9753
R_L			
Temkin			
A	2.0398×10^{-8}	1.8935×10^{-8}	4.696×10^{-8}
B	2.8230	3.3781	-6.3526×10^{-6}
R^2	0.8390	0.9084	0.4984

Table 3.
 Equilibrium parameters of adsorption models at different temperatures for Co ions.

[4, 5, 13], However, other authors agree with that found in this work, where the heat of adsorption is positive and, as the temperature of the process increases, the adsorption of the ions in the material increases [32].

3.3 Effect of contact time and amount of adsorbent

In the process of solid-liquid adsorption, it is convenient to know the necessary contact time between the adsorbent and the adsorbate to achieve a maximum interaction between both and get removed as much metal ions as possible. **Figures 4–6** show the adsorption curves of each metal ion, where it is observed that about 10 h after the start of the process, the adsorption speed is high and that after this time the rate of removal of the ions. It decays, probably, because the sites where the capture of the ions is carried out are saturated, and therefore the balance is reached regardless of the concentration of absorber that has been used. This type of behavior is common among various adsorbent materials [37]. Also, it is observed that the adsorption capacity of the adsorbent material decreases significantly with the

Models	Parameters		
	15°C	30°C	45°C
SIPS			
K_S	1.396×10^{-5}	ND	0.2080
q_m	41.4493		41.3266
n_S	2.3971		1.1676
R^2	0.9980		0.9200
Redlich-Peterson			
K_R	0.2036	ND	9.9421
a_R	0.0013		0.2322
β	1.0		1.0
R^2	0.9632		0.9170
Langmuir			
K_L	0.0013	ND	0.2322
q_m	154.8825		42.8164
R^2	0.9632		0.9170
R_L	0.435–0.885		0.004–0.041
Freundlich			
K_F	0.2914	ND	14.5249
n	1.1274		4.7001
R^2	0.9548		0.7741
Temkin			
A	2.9527×10^{-8}	ND	10.1004
B	4.5983		6.7337
R^2	0.5789		0.8472

Table 4.
Equilibrium parameters of adsorption models at different temperatures for Cu ions.

Metal	T (K)	$-\Delta G$ (kJ/mol)	ΔH (kJ/mol)	ΔS (kJ/mol K)
Ni	288.15	18.52	69.63	308.53
	303.15	25.56		
	318.15	27.62		
Co	288.15	24.15	13.39	130.08
	303.15	25.91		
	318.15	28.07		
Cu	288.15	20.20	131.74	572.27
	303.15	ND		
	318.15	36.02		

Table 5.
Thermodynamic parameters for the equilibrium adsorption process of Ni, Co, and Cu ions.

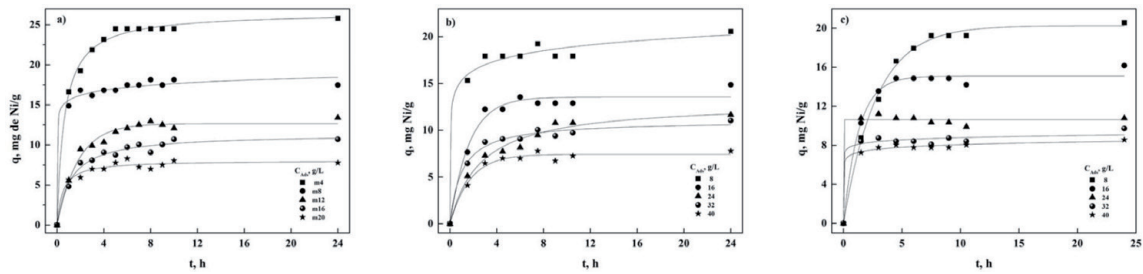


Figure 4.
 Behavior of the removal of Ni ions at different temperatures and concentrations of adsorbent: (a) 15, (b) 30 and (c) 45°C.

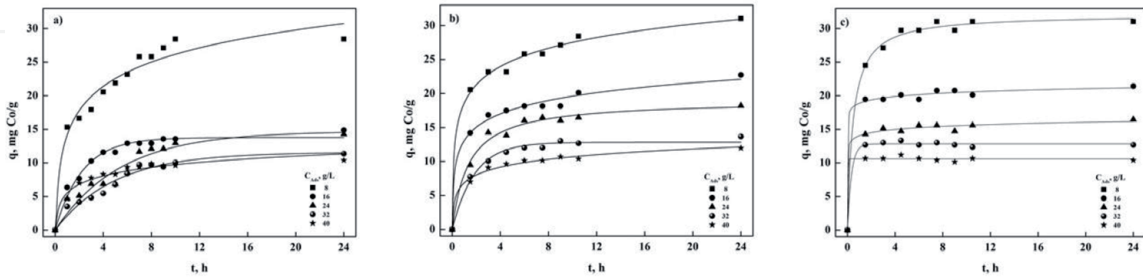


Figure 5.
 Behavior of the removal of Co ions at different temperatures and concentrations of adsorbent: (a) 15, (b) 30 and (c) 45°C.

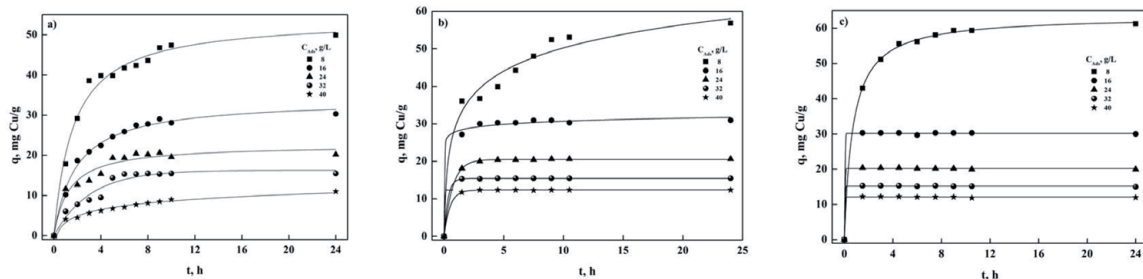


Figure 6.
 Behavior of the removal of Cu ions at different temperatures and concentrations of adsorbent: (a) 15, (b) 30 and (c) 45°C.

increase in the concentration of adsorbent independent of the temperature at which the removal process is carried out, so that the adsorption potential of the Ni ions decreases from 25.8 to 7.78 mg/g at 15°C, while at 30 and 45°C, it decreases from 20.6 to 7.78 and 20.6 to 8.6 mg/g, respectively. In the case of Co ions, the adsorption capacity decreases from 28.4 to 10.4 mg/g, from 31.04 to 11.97 mg/g, and from 31.04 to 10.4 mg/g at 15, 30, and 45°C, respectively. Finally, in the case of Cu ions, the decrease in the adsorption capacity at 15, 30, and 45°C was 49.9–11.0, 56.8–12.4, and 61.2–12 mg/g, respectively. This type of behavior is observed in the adsorption of metals [1, 26, 28, 29].

In the aqueous solutions with the three metal ions present, a behavior similar to that observed in the solutions prepared with a single metal compound was observed; however, the time necessary to reach equilibrium was around 5 h, and the adsorption capacity of the ions in solution was also significantly decreased by increasing the concentration of sorbent in the solution. The adsorption capacity achieved (**Figure 7**), for Ni ions, was from 32.4 to 6.2 mg/g, for Co ions from 41.9 to 10 mg/g, and for Cu ions from 59.9 to 12.1 mg/g at 45°C, which indicates that

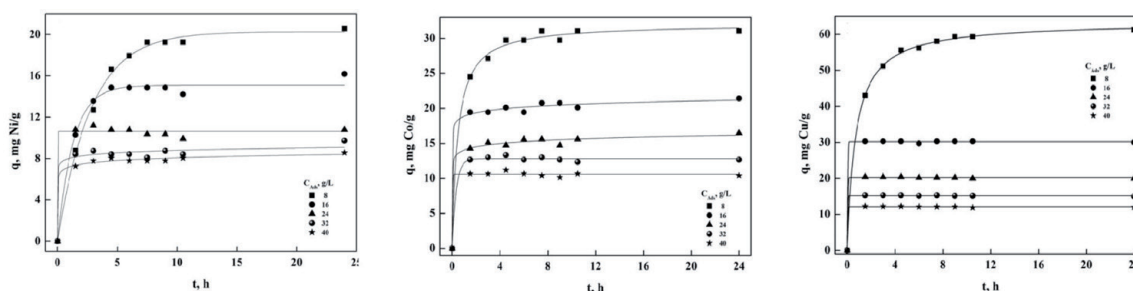


Figure 7. Behavior of the different metallic ions of Ni, Co, and Cu found in the solution at 45°C.

it is not necessary to saturate the solution with nDCPD to achieve greater metal uptake [32–34]. On the other hand, in the analysis of the Co-Cu binary solution, a behavior similar to the previous cases was observed, achieving a greater adsorption capacity with less amount of adsorbent, so that at a temperature of 45°C (**Figure 8**), for Co ions, it was possible to adsorb 32–9.9 mg/g and for Cu ions from 57 to 11.8 mg/g.

In the removal of ions in solutions, it was observed that the percentage of removal increases with the increase in the amount of nDCPD used, achieving removal percentages close to 100% for Cu ions and 95% for Co ions; however, for Ni about 70% removal was only achieved (**Figure 9**), suggesting that sites available for nickel capture are quickly saturated due to the large amount of chromium in the effluent. The changes caused by the variation of the temperature depend on the metal ion, since the maximum removal of the Ni ions is between 15 and 30°C, while for the Cu and Co ions, it is given at 30°C. Similar observations have been reported in adsorption studies conducted with other biomaterials [29, 38]. The selectivity shown in the present study was the following: Cu > Co > Ni, with percentages of removal in solutions composed of the three ions of 96% (Cu), 83% (Co), and 59% (Ni). Additionally, in **Figure 10**, it is observed that in the solutions composed only by Co or Cu, the time necessary to reach the equilibrium decreases considerably; in addition, the selectivity is maintained toward the removal of Cu compared to the Co, having a percentage of removal of 95–79%, respectively. Finally, the changes caused by the variation of the temperature depend on the metal ion, since the maximum removal of the Ni ions is between 15 and 30°C, while for the Cu and Co ions, it was at 30°C (**Figure 11**).

3.4 Kinetic study

To understand the process of removal of the different metal ions in aqueous solution, as well as the relationship that occurs between the metals and the interaction of the metal ions with the adsorbent material, the data obtained in the experimentation was evaluated at different temperatures and with different concentrations of adsorbents with the adsorption models that are concentrated in **Table 6** [6]. The kinetic parameters calculated with the different models (**Table 1**), were used to adjust the experimental adsorption values obtained for the three metal ions with the different concentrations of adsorbent and temperatures utilized, by using SigmaPlot software (Version 11®). Based on the obtained values, it is distinguished that the models that present the best adjustments to the obtained data are pseudo first order, Elovich and pseudo-second order, so it can be inferred that the removal mechanism is due to the ions being adsorbed in one or two sites on the surface that is heterogeneous since each site has different adsorption energy

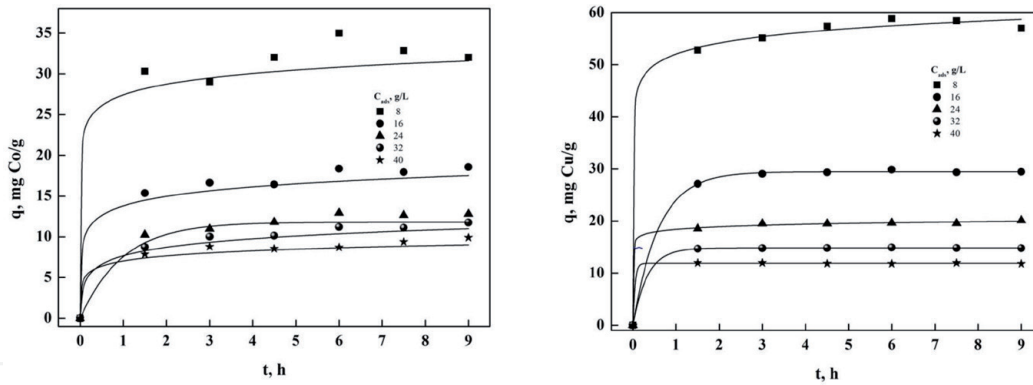


Figure 8.
 Behavior of the different metal ions of Co and Cu found in the solution at 45°C.

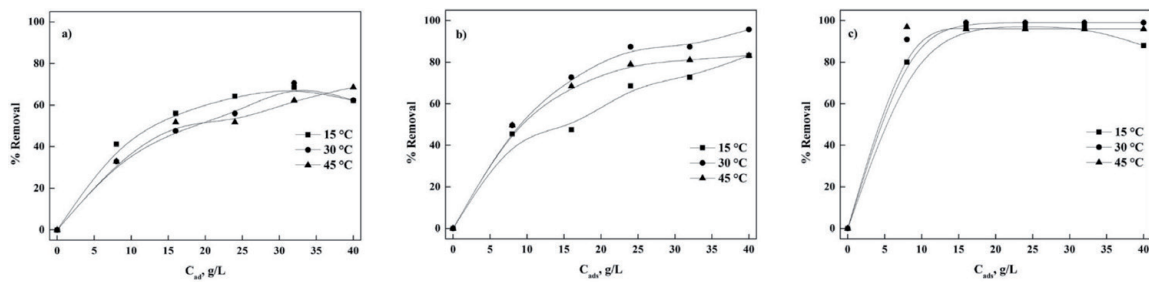


Figure 9.
 Removal of the different metals in aqueous solution at 15, 30, and 45°C.

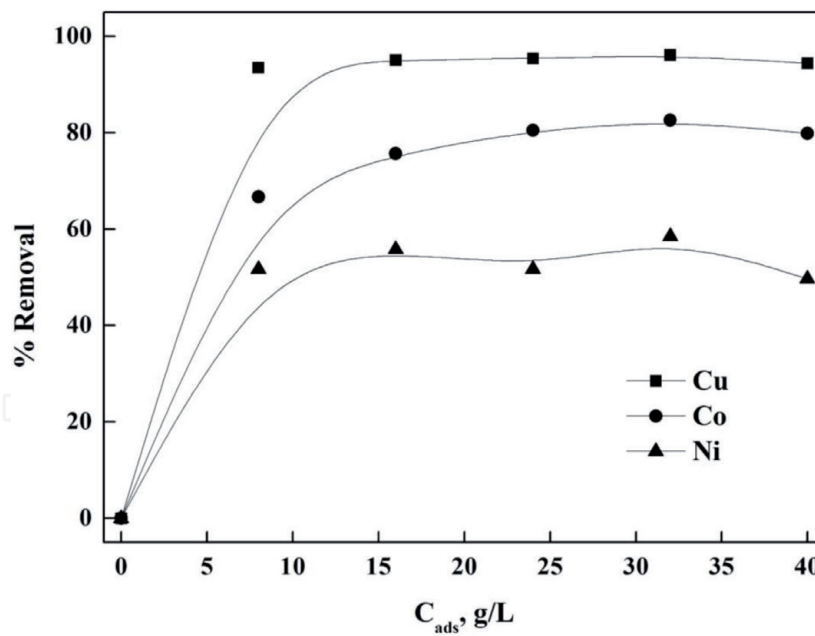


Figure 10.
 Removal of Cu, Co, and Ni ions that are in the same solution at 45°C.

[1, 4, 5]. Similarly, it can be noticed that the models that do not adequately describe the process of metal removal in nDCPD are those that are related to the mass transfer both external and internal, independent of the temperature, the concentration of the adsorbent material, and the presence of another metal ion in the same solution; so it can be inferred that the removal process of these metals does not present problems of mass transfer.

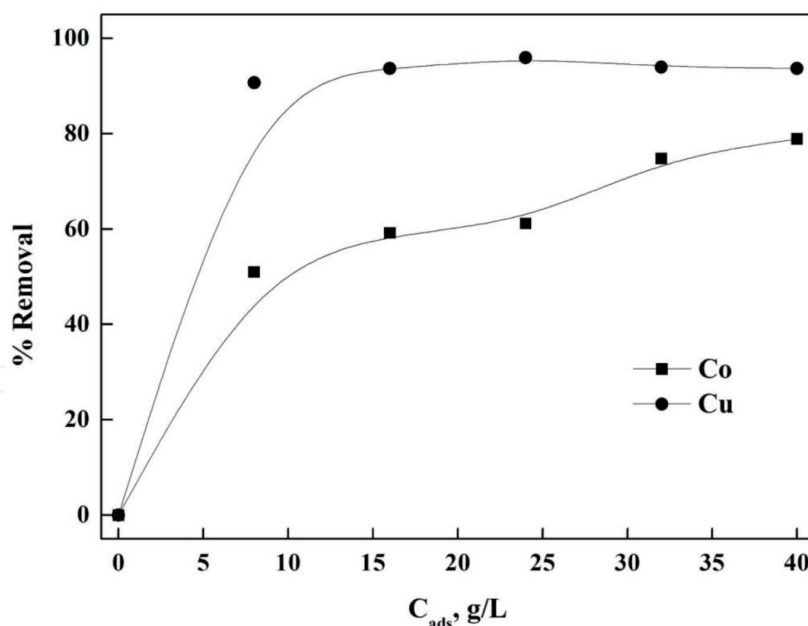


Figure 11.
Removal of Cu and Co ions in the aqueous solution at 45°C.

Model	Equation	Ref.
Pseudo-first order	$\frac{dq}{dt} = k_1(q_e - q)$	[35]
Pseudo-second order	$\frac{dq}{dt} = k_2(q_e - q)^2$	
Elovich	$\frac{dq}{dt} = \alpha e^{-\beta q}$	
Intraparticle diffusion (DI)	$q = k_{id}t^{0.5}$	
External diffusion (DE)	$\ln\left(\frac{C}{C_0}\right) = -k_{ext}t$	[37]

Table 6.
Adsorption isotherm models used for the analysis of experimental data.

3.5 Characterization of nDCPD

Figure 12 shows the SEM image of the nDCPD doped with the Ni, Co, and Cu ions, where the main characteristics of nDCPD (**Figure 12a**), monoclinic disk morphology [1, 15, 29, 39], which does not present significant changes in the presence of Ni (**Figure 12b**), Co (**Figure 12c**), and Cu (**Figure 12d**) ions can be observed, probably because the vast majority of metal ions are adsorbed on the surface of nDCPD. The XRD patterns of nDCPD doped with Ni, Co, and Cu are shown in **Figure 13**, and according to the International Center of Diffraction Data Chart (JCPDS) database, some changes are observed in the samples with metal ions compared to that of nDCPD without doping [1]. The peaks at $\sim 32^\circ$ and 40° increase in intensity, while at $\sim 34^\circ$, the intensity of the peaks directly related to the presence of Ni, Co, and Cu ions decreases. While at 26, 29, and 53° , new peaks appear in the doped brushite samples, which also caused a decrease in the network parameter of 4.99 nm, a value lower than the 5.77 nm obtained for nDCPD, without doping, together with the particle size from 9.26 to 4.45, 4.08, and 4.35 Å, for Ni, Co, and Cu, respectively, which was determined with the Scherrer Equation [39, 40]. This may be due to the fact that the Ca ions of nDCPD without doping (1.12 Å) are replaced during the adsorption process by the ions of Ni (0.78 Å), Co (0.63 Å), and Cu (0.69 Å), which implies that part of the ions are retained inside the structure of nDCPD [40].

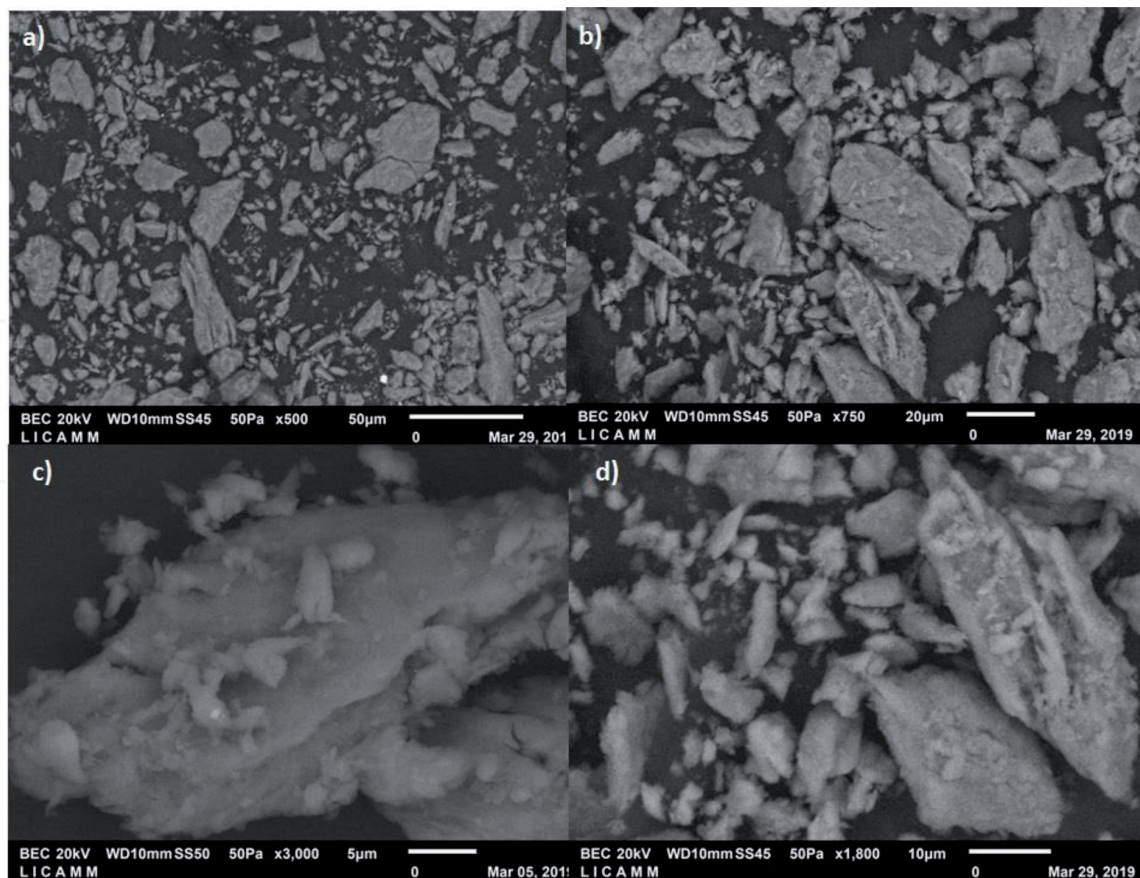


Figure 12.
Micrographs obtained in SEM: (a) brushite, (b) Ni, (c) Co, and (d) Cu.

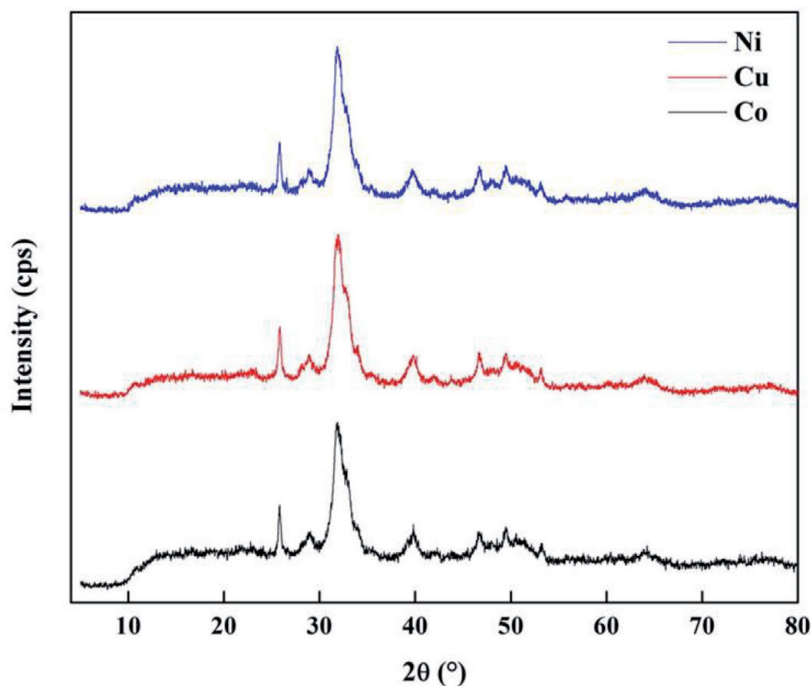


Figure 13.
X-ray diffraction patterns of nCDPD doped with the different metal ions.

In **Figure 14**, the infrared spectra of nCDPD are presented, where the characteristic peaks of the groups that make up apatite are observed, among which the presence of a doublet stands out at 577 and 526 cm^{-1} , characteristic of the vibrations of flexing of the phosphate groups; while the signal at 790 cm^{-1} is due to bending out of the P-O-H plane; at 987 and 873 cm^{-1} , there are peaks related to

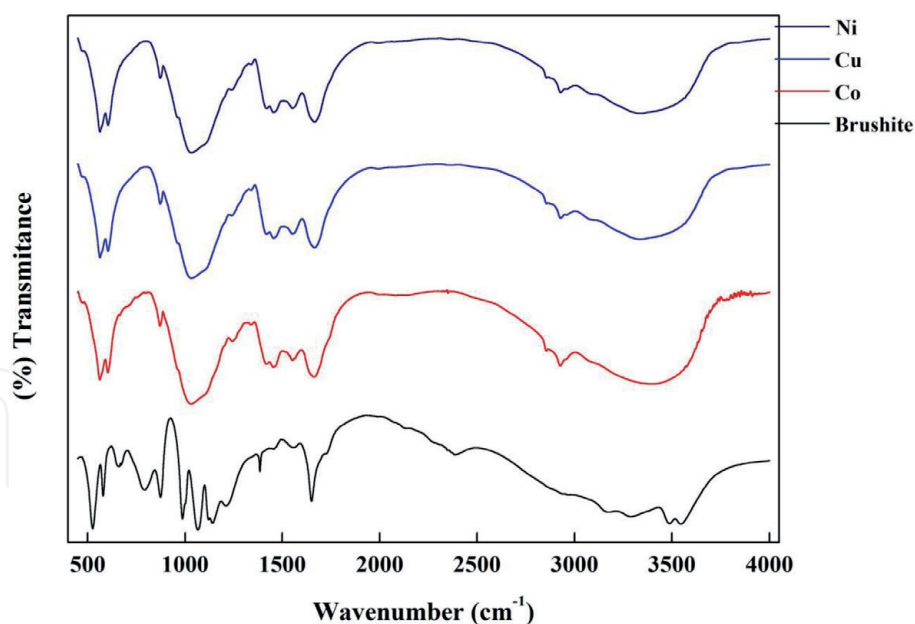


Figure 14.
Infrared spectrum of pure nDCPD doped with Ni, Co, and Cu.

the stretching of P-O (H) in the HPO_4^{2-} . On the other hand, the signals found at 1138, 1120, 1065, and 1004 cm^{-1} are attributed to the stretching of the P-O link. At 1215 cm^{-1} the signal generated by the flexion of the O-H group plane is presented, and the peaks observed at 665 and 1651 cm^{-1} are related to the binding vibrations and physical vibrations of the water molecule. Additionally, a shoulder at 1725 cm^{-1} was observed, which is related to the flexural stress of the water molecule, and the signals obtained at 3548, 3484, 3278, and 3166 cm^{-1} are related to the extension of the water molecule in the apatite. Finally, a band at 2944 cm^{-1} was also observed, directly related to the stretching of PO-H that occurs in HPO [1, 41, 42]. In the case of the nDCPD spectra with the different metal ions, it was observed that several peaks decrease in intensity or disappear as a result of the presence of Ni, Co, and Cu; these signals are related to the PO_4^{3-} and OH groups, with which it can be inferred that the groups present on the surface of this apatite participate in the adsorption of metals directly.

4. Conclusion

Based on the thermodynamic parameters obtained at different temperatures and concentrations of brushite (nDCPD), used as an adsorbent material in the removal of different heavy metals (Ni, Co, and Cu), from aqueous solutions, it can be concluded that the adsorption of heavy metals with nDCPD is feasible and that the adsorption capacity of nDCPD increases at a higher temperature. The percentages of removal achieved show that nDCPD has a higher affinity for adsorbing Cu and Co compared to Ni. From the data obtained from the adsorption isotherms, it can be inferred that the process of removing the metal ions in solution on the surface of nDCPD is carried out, forming a heterogeneous monolayer since the model that best fits to the data obtained in the SIPS is a combination of the Langmuir and Freundlich models. The experimental data obtained also show that there are different models to describe the kinetic process of adsorption, such as the pseudo-first-order model, which suggests that only one surface site is needed for adsorption to take place, as well as the pseudo-second-order model which indicates that two sites are needed for each ion molecule and that each site requires different adsorption

energies as described by the Elovich model, which confirms the heterogeneity of the nDCPD surface determined from the adsorption isotherms generated. The surface changes of nDCPD, evidenced by the XRD and FTIR analyses, suggest that the HPO^- and PO_4^{3-} are directly involved in the Ni, Co, and Cu adsorption process, which allows us to conclude that nDCPD is an appropriate candidate to be used in the removal of heavy metals present in wastewater from different industries.

Acknowledgements

The authors thank the Interdisciplinary Professional Unit of Engineering Campus Guanajuato of the IPN, the Center for Nanoscience and Nanotechnology (CNyN) of the UNAM, and the Colombian Polytechnic “Jaime Isaza Cadavid” for the infrastructure provided for the realization of this project and the Research and Postgraduate Secretary for the financial support for this work (SIP: 20170577) and to the BIOCATEM Network.

Author details

Rosa Hernández-Soto^{1*}, José A. Hernández¹, Alba N. Ardila-Arias², Mercedes Salazar-Hernández³ and María del Carmen Salazar-Hernández⁴

¹ Instituto Politécnico Nacional, UPIIG, Guanajuato, Mexico

² Grupo de Investigación en Química Básica y Aplicada a Procesos Bioquímicos, Biotecnológicos y Ambientales, Politécnico Colombiano Jaime Isaza Cadavid, Medellín, Colombia

³ Departamento de Ingeniería en Minas, Metalurgia y Geología, División de Ingenierías, Universidad de Guanajuato, Guanajuato, Mexico

⁴ Departments of Materials Science, Chemistry, Environmental Science, Earth and Planetary Sciences, UPIIG - Instituto Politécnico Nacional Unidad Profesional Interdisciplinaria De Ingeniería Campus Guanajuato, Silao de la Victoria, Guanajuato, Mexico

*Address all correspondence to: rosyhdezs@yahoo.com

IntechOpen

© 2019 The Author(s). Licensee IntechOpen. This chapter is distributed under the terms of the Creative Commons Attribution License (<http://creativecommons.org/licenses/by/3.0>), which permits unrestricted use, distribution, and reproduction in any medium, provided the original work is properly cited. 

References

- [1] Hernández-Maldonado JA, Torres-García FA, Salazar-Hernández MM, Hernández-Soto R. Removal of chromium from contaminated liquid effluents using natural brushite obtained from bovine bone. *Desalination and Water Treatment*. 2017;**95**:262-273. DOI: 10.5004/dwd.2017.21480
- [2] Yildiz S. Kinetic and isotherm analysis of Cu(II) adsorption onto almond shell (*Prunus dulcis*). *Ecological Chemistry and Engineering S*. 2017;**24**(1):87-106. DOI: 10.1515/eces-2017-0007
- [3] Moreira VR, Lebron YAR, Freire SJ, Santos LVS, Palladino F, Jacob RS. Biosorption of copper ions from aqueous solution using *Chlorella pyrenoidosa*: Optimization, equilibrium and kinetics studies. *Microchemical Journal*. 2019;**145**:119-129. DOI: 10.1016/j.microc.2018.10.027
- [4] Giza S. Biosorption of heavy metal from aqueous waste solution using cellulosic orange peel. *Ecological Engineering*. 2017;**99**:134-140. DOI: 10.1016/j.ecoleng.2016.11.043
- [5] Sudha R, Srinivasan K, Premkumar P. Removal of nickel(II) from aqueous solution using Citrus Limettioides peel and seed carbon. *Ecotoxicology and Environmental Safety*. 2015;**117**:115-123. DOI: 10.1016/j.ecoenv.2015.03.025
- [6] Qiu Y, Yang L, Huang S, Ji Z, Li Y. The separation and recovery of copper(II), nickel(II), cobalt(II), zinc(II), and cadmium(II) in a sulfate-based solution using a mixture of Versatic 10 acid and Mextral 984H. *Chinese Journal of Chemical Engineering*. 2017;**25**:760-767. DOI: 10.1016/j.cjche.2016.10.013
- [7] Guo Y, Zhao H, Han Y, Liu X, Guan S, Zhang Q, et al. Simultaneous spectrophotometric determination of trace copper, nickel, and cobalt ions in water samples using solid phase extraction coupled with partial least squares approaches. *Spectrochimica Acta Part A: Molecular and Biomolecular Spectroscopy*. 2017;**173**:532-536. DOI: 10.1016/j.saa.2016.10.003
- [8] Huan-Ping C, Chung-Cheng C, Aileen N. Biosorption of heavy metals on *Citrus maxima* peel, passion fruit shell, and sugarcane bagasse in a fixed-bed column. *Journal of Industrial and Engineering Chemistry*. 2014;**20**:3408-3414. DOI: 10.1016/j.jiec.2013.12.027
- [9] Pedrosa Xavier AL, Herrera Adarme OF, Furtado LM, Dias Ferreira GM, Mendes da Silva LH, Alves Gurgel LV, et al. Modeling adsorption of copper(II), cobalt(II) and nickel(II) metal ions from aqueous solution onto a new carboxylated sugarcane bagasse. Part II: Optimization of monocomponent fixed-bed column adsorption. *Journal of Colloid and Interface Science*. 2018;**516**:431-445. DOI: 10.1016/j.jcis.2018.01.068
- [10] Qiu X, Hu H, Yang J, Wang C, Cheng Z. Removal of trace copper from simulated nickel electrolytes using a new chelating resin. *Hydrometallurgy*. 2018;**180**:121-131. DOI: 10.1016/j.hydromet.2018.07.015
- [11] Liu X, He Y, Zhao Z, Chen X. Study on removal of copper from nickel-copper mixed solution by membrane electrolysis. *Hydrometallurgy*. 2018;**180**:153-157. DOI: 10.1016/j.hydromet.2018.07.019
- [12] Sikder T, Rahman M, Jakariya M, Hosokawa T, Kurasaki M, Saito T. Remediation of water pollution with native cyclodextrins and modified cyclodextrins: A comparative overview and perspectives. *Chemical Engineering Journal*. 2019;**355**:920-941. DOI: 10.1016/j.cej.2018.08.218

- [13] Ivanets AI, Srivastava V, Kitikova NV, Shashkova IL, Sillanpää M. Kinetic and thermodynamic studies of the Co(II) and Ni(II) ions removal from aqueous solutions by Ca-Mg phosphates. *Chemosphere*. 2017;**171**:348-354. DOI: 10.1016/j.chemosphere.2016.12.062
- [14] Vollprecht D, Mischitz R, Krois LM, Sedlazeck KP, Müller P, Olbrich T, et al. Removal of critical metals from waste water by zero-valent iron. *Journal of Cleaner Production*. 2019;**208**:1409-1420. DOI: 10.1016/j.jclepro.2018.10.180
- [15] Martins JJ, Órfão JJM, Soares OGSP. Sorption of copper, nickel and cadmium on bone char. *Protection of Metals and Physical Chemistry of Surfaces*. 2017;**53**(4):618-627. DOI: 10.1134/S2070205117040153
- [16] Moscatello NJ, Pfeifer BA. Yersiniabactin metal binding characterization and removal of nickel from industrial wastewater. *Biotechnology Progress*. 2017;**33**(6):1548-1554. DOI: 10.1002/btpr.2542
- [17] Osińska M. Removal of lead(II), copper(II), cobalt(II) and nickel(II) ions from aqueous solutions using carbon gels. *Journal of Sol-Gel Science and Technology*. 2017;**81**:678-692. DOI: 10.1007/s10971-016-4256-0
- [18] Bhatnagar A, Sillanpää M. Utilization of agro-industrial and municipal waste materials as potential adsorbents for water treatment: A review. *Chemical Engineering Journal*. 2010;**157**:277-296. DOI: 10.1016/j.cej.2010.01.007
- [19] Bhatnagar A, Sillanpää M, Witek-Krowiak A. Agricultural waste peels as versatile biomass for water purification: A review. *Chemical Engineering Journal*. 2015;**270**:244-271. DOI: 10.1016/j.cej.2015.01.135
- [20] Romero-Cano LA, García-Rosero H, Gonzalez-Gutierrez LV, Baldenegro-Pérez LA, Carrasco-Marín F. Functionalized adsorbents prepared from fruit peels: Equilibrium, kinetic and thermodynamic studies for copper adsorption in aqueous solution. *Journal of Cleaner Production*. 2017;**162**:195-204. DOI: 10.1016/j.jclepro.2017.06.032
- [21] Femina Carolin C, Senthil Kumar P, Saravanan A, Janet Joshiba G, Naushad M. Efficient techniques for the removal of toxic heavy metals from aquatic environment: A review. *Journal of Environmental Chemical Engineering*. 2017;**5**:2782-2799. DOI: 10.1016/j.jece.2017.05.029
- [22] Liang S, Guo X, Feng N, Tian Q. Adsorption of Cu²⁺ and Cd²⁺ from aqueous solution by mercapto-acetic acid modified orange peel. *Colloids and Surfaces B: Biointerfaces*. 2009;**73**:10-14. DOI: 10.1016/j.colsurfb.2009.04.021
- [23] Annadurai G, Juang RS, Lee DJ. Adsorption of heavy metals from water using banana and orange peels. *Water Science and Technology*. 2002;**47**(1):185-190. DOI: 10.2166/wst.2003.0049
- [24] De Gisi S, Lofrano G, Grassi M, Notarnicola M. Characteristics and adsorption capacities of low-cost sorbents for wastewater treatment: A review. *Sustainable Materials and Technologies*. 2016;**9**:10-40. DOI: 10.1016/j.susmat.2016.06.002
- [25] Romero-Cano LA, Gonzalez-Gutierrez LV, Baldenegro-Perez LA. Biosorbents prepared from orange pressure peels using instant controlled drop for Cu(II) and phenol removal. *Industrial Crops and Products*. 2016;**84**:344-349. DOI: 10.1016/j.indcrop.2016.02.027
- [26] Moreno-Piraján JC, Giraldo L. Heavy metal ions adsorption from wastewater using activated carbon from orange peel. *E-Journal of Chemistry*. 2012;**9**(2):926-937. DOI: 10.1155/2012/928073

- [27] Farroq U, Kozinski JA, Ain Khan M, Athar M. Biosorption of heavy metal ions wheat based biosorbents—A review of the recent literature. *Bioresource Technology*. 2010;**101**:5043-5053. DOI: 10.1016/j.biortech.2010.02.030
- [28] Habib A, Islam N, Islam A, Shafiqul Alam AM. Removal of copper from aqueous solution using orange peel, sawdust and bagasse. *Pakistan Journal of Analytical & Environmental Chemistry*. 2007;**8**(1-2):21-25. DOI: 10.21743/pjaec/2016.06.005
- [29] Khalfaoui A, Meniai AH. Application of chemically modified orange peels for removal of copper(II) from aqueous solutions. *Theoretical Foundations of Chemical Engineering*. 2012;**46**(6):732-739. DOI: 10.1134/S0040579512060103
- [30] Surovka D, Pertile E. Sorption of iron, manganese, and copper from aqueous solution using orange peel: Optimization, isothermic, kinetic, and thermodynamic studies. *Polish Journal of Environmental Studies*. 2017;**26**(2):795-800. DOI: 10.15244/pjoes/60499
- [31] Hamidi E, Arsalane S, Halim M. Kinetics and isotherm studies of copper removal by brushite calcium phosphate: Linear and non-linear regression comparison. *E-Journal of Chemistry*. 2012;**9**(3):1532-1542. DOI: 10.1155/2012/928073
- [32] Mobasherpour I, Salahi E, Pazouki M. Comparative of the removal of Pb^{2+} , Cd^{2+} and Ni^{2+} by nano crystallite hydroxyapatite from aqueous solutions: Adsorption isotherm study. *Arabian Journal of Chemistry*. 2012;**5**:439-446. DOI: 10.1016/j.arabjc.2010.12.022
- [33] El Hamidi A, Mulongo Masamba R, Khachani M, Halim M, Arsalane S. Kinetics modeling in liquid phase, sorption of copper ions on brushite di-calcium phosphate dihydrate $CaHPO_4 \cdot 2H_2O$ (DCPD). *Desalination and Water Treatment*. 2016;**56**:779-791. DOI: 10.1080/19443994.2014.940391
- [34] Huang Y, Chen L, Wang H. Removal of Co(II) from aqueous solution by using hydroxyapatite. *Journal of Radioanalytical and Nuclear Chemistry*. 2012;**291**:777-785. DOI: 10.1007/s10967-011-1351-0
- [35] Fernane F, Boudia S, Aiouache F. Removal Cu(II) and Ni(II) by natural and synthetic hydroxyapatites: A comparative study. *Desalination and Water Treatment*. 2014;**52**:2856-2862. DOI: 10.1080/19443994.2013.807084
- [36] Singh KK, Hasan SH, Talat M, Singh VK, Gangwar SK. Removal of Cr(VI) from aqueous solutions using wheat bran. *Chemical Engineering Journal*. 2009;**151**:113-121. DOI: 10.1016/j.ccej.2009.02.003
- [37] Elabbas S, Mandi L, Berrekhis F, Pons MN, Leclerc JP, Ouazzani N. Removal of Cr(III) from chrome tanning wastewater by adsorption using two natural carbonaceous materials: Eggshell and powdered marble. *Journal of Environmental Management*. 2016;**166**:589-595. DOI: 10.1016/j.jenvman.2015.11.012
- [38] Pehlivan E, Pehlivan E, Tutor-Kahraman H. Hexavalent chromium removal by Osage Orange. *Food Chemistry*. 2012;**133**:1478-1484. DOI: 10.1016/j.foodchem.2012.02.037
- [39] Mirković MM, Lazarević-Pašti TD, Došen AM, Čebela MŽ, Rosić AA, Matović BZ, et al. Adsorption of malathion on mesoporous monetite obtained by mechanochemical treatment of brushite. *RSC Advances*. 2016;**6**:12219-12225. DOI: 10.1039/c5ra27554g
- [40] Thangadurai V, Kopp P. Chemical synthesis of Ca-doped CeO_3 -intermediate temperature oxide ion

electrolytes. *Journal of Power Sources*.
2007;**168**:178-183. DOI: 10.1016/j.
jpowsour.2007.03.030

[41] Sopcak T, Medvecký L, Giretova
M, Stulajterona R, Durisin J, Girman
V, et al. Effect of phase composition
of calcium silicate phosphate
component on properties of brushite
based composite cements. *Materials
Characterization*. 2016;**117**:17-29. DOI:
10.1016/j.matchar.2016.04.011

[42] Arifuzzaman SM, Rohani S.
Experimental study of brushite
precipitation. *Journal of Crystal
Growth*. 2004;**267**:624-634. DOI:
10.1016/j.crysgro.2004.04.024

IntechOpen